Proceedings of 20th International Congress on Acoustics, ICA 2010

23-27 August 2010, Sydney, Australia

Multisource industrial plant inverse noise modelling and assessment against ISO 8297

Daniel Castro Cirac (1), Jorge Reverter García (2), Michael Kidner (3)

(1) VIPAC Engineers & Scientists Ltd., Sydney, Australia
(2) Planifica Urbanismo y Gestión S.L., Castelló, Spain
(3) VIPAC Engineers & Scientists Ltd., Adelaide, Australia

PACS: 43.60.Pt, 43.20.Ye, 43.50.Yw, 43.58.Ta

ABSTRACT

A number of situations may occur where multiple industrial noise sources combine to produce troublesome acoustic environments. In some cases, industrial activity develops adjacent to residential areas creating the need for control of noise propagation to its surroundings. In addition, the same industrial site could have a noise issue within the facility that may be of interest for health and safety of personnel. In the former scenario, ISO 8297 "Determination of acoustic power levels of multisource industrial plants for evaluation of sound pressure levels in the environment" has been used to predict the far field noise generated by industrial plants. This approach has proven to be useful where the required criteria are set in terms of acoustic power levels and only one single result value is expected for the whole plant. However, in the event that mitigation is required to control noise at residential receivers or for health and safety reasons, a more detailed method is needed to enable source identification and ranking of the relevant noise sources. This paper presents an alternative method that allows obtaining the acoustic power levels of the individual noise sources using inverse theory applied to noise modelling. This process is achieved by means of measurements of sound pressure levels around the noise sources and noise propagation modelling. Even though this method is well known, its application to real cases relies heavily on a combination of the quality of the measured data and the physical conditions of the problem. Thus, the numerical process usually involves the solution of ill-conditioned matrices that require regularisation in order to achieve stable results. This paper presents a practical example of the application of both methods in a real scenario highlighting the advantages and disadvantages of the two.

INTRODUCTION

Some of the benefits of a modern life such as transport, industry, heating and cooling, demand a stable, secure and continuous supply of energy. Despite the recent price fluctuations and economic growth, the annual average growth in energy consumption in Australia has remained around 2.3 per cent during the past five decades [1]. This need for energy has contributed to the increasing number of power station developments including coal plants, gas turbines, hydroelectric, wind farms, biomass and cogeneration plants.

One of the many aspects of the environmental impact assessment process associated with the aforementioned facilities is the prediction of their noise impacts. Therefore, all these developments pose a challenge to achieve a balance between operational performance and minimizing any adverse impact to the facilities surroundings. The noise impact is usually taken into account during design and planning approval stages in order to gauge and prevent any potential problems during both construction and operational stages.

Methods to evaluate noise emissions from industrial plants are listed in a comprehensive set of international standards such as ISO, DIN (German Institute for Standardisation) or VDI (Association of German Engineers) such as the standards listed on [2, 3 and 4]. Usually, a client will explicitly require assessments to be carried out according to those standards. However, due to some of the constraints contained in the standards, alternative methods can be sought to step away from conventional procedures in order to seek another effective way to solve a specific problem.

This paper deals with the comparison of two methods to analyse the noise environment created by multisource industrial plants in proximity to residential areas. Additionally, one of the methods has been found useful when applied to evaluate and improve the occupational noise environment of a plant. In summary, we present inverse noise modelling [5, 6, 7] as an alternative methodology to ISO standard 8297 [8] in terms of determining the acoustic power of large industrial plants.

The remainder of the paper is structured as follows: description of ISO standard 8297 and its methodology; brief description of inverse noise modelling theory and its application to acoustics and development of a real case scenario where the two methods have been applied. Finally, the conclusions present a summary of the advantages and handicaps of the two methods.

ISO STANDARD 8297

ISO 8297 is an engineering method (grade 2) standard that deals with sound pressure and acoustic power levels generated by industrial plants. This method offers the possibility of obtaining the acoustic power of the entire plant by conducting sound pressure measurements at specific control points located at the perimeter of the plant. The results are sufficient if receiver distances are far larger than the dimensions of the plant or if the requirements are set only as a single value of acoustic power level for the entire facility.

Procedure

Several microphone positions have to be defined along a closed line path around the plant area (see Figure 1). These locations must comply with a series of requirements in regards of the dimensions of the plant, the control measurements distances between each other and the angles of each control point in respect the whole plant area.

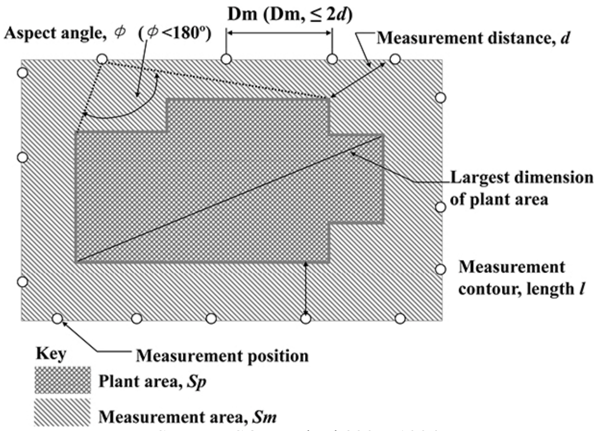

Source: ISO standard 8297, 1994

Figure 1. General arrangement of contour measurement positions around the plant

The sound pressure values measured at control points, conducted in general accordance with [8 and 9], are logarithmically averaged and corrected for background noise and atmospheric attenuation. The resulting single value could be then used either to compare it with the criteria or as input data in a noise propagation software model.

Using a plot plan, scale drawing or similar it is very helpful to define the points and double-check its adequacy. It is anticipated that several iterations will be need in order to comply with all requirements of the standard. For this reason, it is recommended to follow this procedure before the noise survey. Once the locations are defined, the measurements will consist of straightforward sound pressure level (SPL) measurements.

Note that the measurements of background noise are to be performed at each measurement location and therefore it is necessary to have the measurement location defined before starting the noise survey.

The atmospheric characteristics of the site are also required to be taken into account, particularly wind speed and direction. If the results of the ISO standard 8297 are expected to be incorporated in noise propagation software, the atmospheric effects will play a major role at large distances from the site as reported by Blake and Teague [10].

Ambiguities and problems

There are a number of unresolved ambiguities in ISO standard 8297 mainly related with the physical characteristics of the site and measurement procedures. For instance, it is not defined what is a high source, what defines if the source needs a separate acoustic power level and, in case it needs it, which procedure needs to be followed to measure it.

In addition, Brittain [11] also reported a problem with formula 10.4 from ISO standard 8297. See equation ($1a$)

$$a)\ \Delta L_S = 10\log_{10}\left(\frac{2S_m+hl}{S_0}\right);\ b)\ \Delta L_S = 10\log_{10}\left(\frac{S_m+hl}{S_0}\right) \quad (1)$$

where ΔL_S is the area term, in dB; S_m is the measurement area in m^2 (see Figure 1); h is the microphone height in metres, l is the length of the measurements contour in metres, and S_0 is a reference area equal to 1 m^2.

The area term is a combination of the wall area (hl) and 2 times the surface S_m equation ($1a$). However, we are of the opinion that only the top side of S_m will be effectively radiating because the bottom will be on the ground, therefore, the formula can be rewritten omitting one of the S_m as per equation ($1b$). This variable is the most significant correction applied to sound pressure measurements and could imply differences up to 3 dB, see equation (16).

INVERSE NOISE MODELLING

Background

An inverse problem can be defined as the process of obtaining model parameters $\boldsymbol{m}$ from observed data $\boldsymbol{d}$ in a physical system using a linear or non-linear operator $\boldsymbol{G}$ which describes the relationship between $\boldsymbol{d}$ and $\boldsymbol{m}$. This can be denoted as

$$\boldsymbol{d} = \boldsymbol{G}(\boldsymbol{m}) \quad (2)$$

In our case, a set of sound sources with unknown acoustic power values $\boldsymbol{m}$ and a set of points with sound pressure values $\boldsymbol{d}$ are related through a combination of an acoustic near and free field radiation $\boldsymbol{G}$. This can be arranged as a discrete linear system, where $\boldsymbol{d}$ and $\boldsymbol{m}$ are vectors at each frequency of analysis f and equation (2) becomes a matrix equation represented as

$$\boldsymbol{d_i(f)} = \boldsymbol{G_{ij}(f)m_j(f)}\ \ \forall\ i = 1 \dots M, j = 1 \dots N, M \geq N \quad (3)$$

$$\begin{bmatrix} \boldsymbol{d_1(f)} \\ \boldsymbol{d_2(f)} \\ \vdots \\ \boldsymbol{d_M(f)} \end{bmatrix} = \begin{bmatrix} \boldsymbol{G_{11}(f)} & \boldsymbol{G_{12}(f)} & \cdots & \boldsymbol{G_{1N}(f)} \\ \boldsymbol{G_{21}(f)} & \boldsymbol{G_{22}(f)} & \cdots & \boldsymbol{G_{2N}(f)} \\ \vdots & \vdots & \ddots & \vdots \\ \boldsymbol{G_{M1}(f)} & \boldsymbol{G_{M2}(f)} & \cdots & \boldsymbol{G_{MN}(f)} \end{bmatrix} \begin{bmatrix} \boldsymbol{m_1(f)} \\ \boldsymbol{m_2(f)} \\ \vdots \\ \boldsymbol{m_N(f)} \end{bmatrix} \quad (4)$$

The number of measurement points M must be greater than set of sources N resulting in a non-squared $\boldsymbol{G(f)}$ matrix, which will not be invertible. There are two important $\boldsymbol{G(f)}$ matrix coefficients characteristics that affect the system solution, namely: the orthogonallity of the rows (i.e. the linear dependence between rows) and the dynamic range of the matrix coefficients (i.e. the difference between the magnitude orders of the coefficients). Several options to regularize ill-conditioned systems are found in the literature [12-16]. Among others, the least-squares method is used to solve the system while introducing probabilistic concepts in order to obtain a stochastic extension of the original deterministic problem.

Assuming measurement or observation of $\boldsymbol{d_i(f)}$ will always carry inherent errors, e.g. exact measurement location, instrument uncertainties, etc., increasing the variability by adding Gaussian noise will contribute to well-pose the problem. Consequently, the solution will be obtained with the contribution of a random process.

Random model parameters solutions will then feed the *forward problem* in order to obtain the error $\boldsymbol{e_i(f)}$ between measured sound pressure values $\boldsymbol{d_i(f)}$ and calculated sound pressure values $\boldsymbol{dc_i(f)}$.

$$\boldsymbol{e_i(f)} = |\boldsymbol{d_i(f)} - \boldsymbol{dc_i(f)}|^2 \tag{5}$$

The solution is then most favourable in the sense that repetition in measurements $\boldsymbol{d_i(f)}$ produces solutions for $\boldsymbol{m_j(f)}$ which, on average, are optimum according to specified error criterion. Nevertheless, the method described here is just one way of obtaining the results among other strategies or analyses that can be used.

Building linear operator *G*(*f*)

As stated in (3), the linear operator $\boldsymbol{G(f)}$ is the relationship between $\boldsymbol{d_i(f)}$ and $\boldsymbol{m_j(f)}$ in a given acoustic field with its own intrinsic radiation properties. In our case $G_{ij}(f)$ can be defined as the ratio of sound pressure squared values at reception point i when source j has unity power and all the other sources are set to zero.

The set of sources $\boldsymbol{m_j(f)}$ were excited with the Kronecker delta δ_{ij}, and the results at receiver points (from frequency octave bands 31.5 Hz to 8 kHz) were used to build up $\boldsymbol{G(f)}$, and feed the mathematical model described in (3).

$$\delta_{ij} = \begin{cases} 1, & \text{if } i = j \\ 0, & \text{if } i \neq j \end{cases} \tag{6}$$

The linear operator $\boldsymbol{G}$ was obtained using a commercial noise propagation software. However, any self-developed model or proprietary software could be used for the same purpose. In our case, a 3D model containing topography, buildings, noise sources and receiver points was implemented in CadnaA and configured to perform noise propagation calculations in accordance with ISO standard 9613 – Part 2 – "Attenuation of sound during propagation outdoors" [2].

Ill-conditioned problem regularisation

One of the main difficulties of dealing with the discrete ill-problem is that $\boldsymbol{G(f)}$ could become a *skinny* linear operator because M is larger than N. Hence, it is necessary to incorporate further information about the solution in order to stabilise the problem and to single out a useful and stable solution. This is the purpose of the regularisation process.

The regularisation of ill-conditioned equations systems is carried out by corrections of the data and/or the linear operators. In our model residual errors exist in each solution of the over-determined system of equations. These errors are solely attributed to the measurements and not to the model which, in its turn, will also add errors that needs to be assumed.

As described in [7 and 14], to minimise the measurement errors Gaussian noise is added to the observed data $\boldsymbol{d}$ and then the system is solved thousands of times. Let the noisy measurements of $\boldsymbol{d_i(f)}$ be denoted as $\boldsymbol{dn_i(f)}$ such that

$$\boldsymbol{dn_{ik}(f)} = \boldsymbol{d_i(f)} + \boldsymbol{\eta_k(f)} \tag{7}$$

where $\boldsymbol{\eta_k(f)}$ represents the Gaussian noise, may be due to measurement error, numerical round off, or uncertainty in the measurement. The substitution of (7) into (2) results in

$$\boldsymbol{dn_{ik}(f)} = \boldsymbol{G_{ij}(f) m_{jk}(f)} + \boldsymbol{\eta_k(f)} \tag{8}$$

This produces k (numbers of samples) matrix solutions in the acoustic power results $\boldsymbol{m_{jk}(f)}$, that represent our stochastic approach to solve the problem.

As stated in [14], among all the normalised probability densities with fixed l_p-norm estimator of dispersion, the one with minimum information content is given by

$$\varphi_p(x) = \frac{p^{1-\frac{1}{p}}}{2\sigma_p \Gamma\left(\frac{1}{p}\right)} e^{-\frac{1}{2}\left(\frac{|x-x_0|p}{(\sigma_p)^p}\right)} \tag{9}$$

where Γ denotes the gamma function and, when p=2, equation (10) becomes

$$\varphi_2(x) = \frac{1}{\sqrt{2\pi\sigma_2}} e^{-\frac{1}{2}\left(\frac{(x-x_0)^2}{\sigma_2{}^2}\right)} \tag{10}$$

and $\varphi_2(x)$ is a Gaussian function, centred at $x=x_0$ with standard deviation equal to σ_2.

Solving the inverse problem

As reported in [7], if Gaussian probability densities are used to model uncertainties, an l_2-norm or least squared criterion is the most efficient way to solve the problem. Hence, assuming the operator $\boldsymbol{G}$ is linear, the probability density $\sigma_m(m)$ when solving (8) is given by the following equation

$$\sigma_m(m) = k\, e^{-\frac{1}{2}\left((m-\tilde{m})^T \tilde{C}_M{}^{-1}(m-\tilde{m})\right)} \tag{11}$$

This implies that $\sigma_m(m)$ is a Gaussian probability density, centred at $\tilde{\boldsymbol{m}}$ with $\tilde{\boldsymbol{C}}_{\boldsymbol{M}}$ as covariance matrix that represents the measure of the linear coupling between each pair of acoustic powers. These values represent the *posteriori* information in the model space, and can be computed using certain matrix identities. This gives

$$\tilde{\boldsymbol{C}}_{\boldsymbol{M}} = \left(\boldsymbol{G}^T \boldsymbol{C_D}^{-1} \boldsymbol{G} + \boldsymbol{C_M}^{-1}\right)^{-1} \tag{12}$$

$$\tilde{\boldsymbol{m}} = \left(\boldsymbol{G}^T \boldsymbol{C_D}^{-1} \boldsymbol{G} + \boldsymbol{C_M}^{-1}\right)^{-1}\left(\boldsymbol{G}^T \boldsymbol{C_D}^{-1} \boldsymbol{d} + \boldsymbol{C_M}^{-1} \boldsymbol{m_{prior}}\right) \tag{13}$$

where $\boldsymbol{C_D}$ is the *a priori* measurements covariance matrix that represents the correlation of the different noise sources simultaneously affecting each single point of measurement. If we do not have any previous information on the model parameters, e.g. acoustic power from manufacturers data sheet or results from on site previous measurements, then we could set $\boldsymbol{C_M} \rightarrow \infty \cdot \mathrm{I}$, so $(\boldsymbol{C_M})^{-1} \rightarrow 0$, and (12) and (13) become

$$\tilde{\boldsymbol{C}}_{\boldsymbol{M}} = \left(\boldsymbol{G}^T \boldsymbol{C_D}^{-1} \boldsymbol{G}\right)^{-1} \tag{14}$$

$$\tilde{\boldsymbol{m}} = \left(\boldsymbol{G}^T \boldsymbol{C_D}^{-1} \boldsymbol{G}\right)^{-1}\left(\boldsymbol{G}^T \boldsymbol{C_D}^{-1} \boldsymbol{d}\right) = \tilde{\boldsymbol{C}}_{\boldsymbol{M}} \left(\boldsymbol{G}^T \boldsymbol{C_D}^{-1} \boldsymbol{d}\right) \tag{15}$$

where $\tilde{\boldsymbol{m}}$ is the solution that generates a set of predicted data closer to the measured data obtained through the least squares estimator and $\tilde{\boldsymbol{C}}_{\boldsymbol{M}}$ represents the influence that each noise source will have upon the rest of the noise sources.

The optimal $\boldsymbol{m_{opt}(f)}$ was determined by solutions that minimised the error function defined in equation (5), i.e. the least squares fit to the measured data at each octave band. Care needs to be taken in order to avoid obtaining negative acoustic powers from (15) assuring the resulting $\boldsymbol{m_{opt}(f)}$ values are always positive.

Additional information such as statistical analysis, graphical data representation and *a posteriori* information from results were included in Matlab scripts in order to validate the accuracy and uncertainties obtained during the numerical process.

CASE HISTORY

Background

As a part of the environmental impact assessment during commissioning a gas delivery station in New South Wales, Australia, required an acoustic assessment to ensure the environmental noise limits were satisfied. Both ISO standard 8297 and inverse noise modelling were used to evaluate the noise impact of the facility.

Description of the site

The gas supply facility is located adjacent to an existing coal fired power station and will provide gas to a new gas fired power station during times of peak consumer demand. In this juncture, the entire facility will operate at the same time, which means that all the noise sources will generate noise simultaneously impeding the identification of the contribution of each individual noise source. The plant can operate any time, day or night, for a maximum of five hours and will operate at the same time as the turbines in the new gas power station.

The site is located adjacent to existing residential communities (R1, R2 and R3). The nearest one (R1) is located 1.3 km. west of the site.

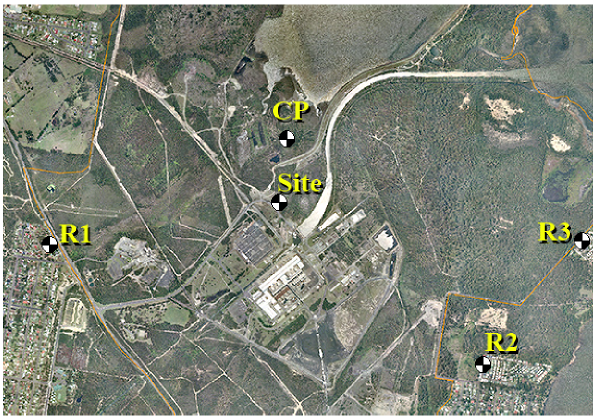

Source: Sixviewer, 2007

Figure 2. Orthophoto of the site location and the receiver points

Criteria

Maximum allowable noise contributions have been determined previously and they are specified in the NSW Department of Planning Project Approval. This criterion also applies to the turbine facility and has been adopted as the benchmark to assess the delivery station. The noise criteria relevant to the nearest noise sensitive locations (residential) under wind speed up to 3 ms^{-1} and temperature inversion conditions of up to $3^{o}C$/100 metres, are contained in Table 1 below.

Table 1. Residential criteria, $L_{Aeq(15min)}$ dBA

Reference time interval	*R1*	*R2*	*R3*
Day (8am-6pm)	40	45	40
Evening (6pm-10pm)	40	45	40
Night (10pm-8am)	40	45	40

Noise sources definition

ISO standard 8297 does not make any reference to the number of noise sources that the plant could contain; however, in order to perform inverse noise modelling one needs to determine how many and which ones are the noise sources expected to be part of the model.

From the documentation received from the client before *in situ* measurements, the following noise sources were identified:

- Water bath heater (x1)
- Emission stacks (x2)
- Centrifugal fans (x2)
- Gas valves regulators (x12)

However, during the noise survey the gas valves were not identified as a noise contributor at all. Instead, few pipe bendings/segments were found as a set of unexpected noise contributors caused by the 90° shifting in the pipe configuration. The water bath heater (BH), the emission stacks (ST), the centrifugal fans (CF) and 5 pipe bending/segments (PB) along the main pipe line were selected as noise sources and became part of the assessment. It is important to highlight the relevance of the selection of the noise sources as this will have a clear implication in the performance of the method. In our case, the modification was based on a combination of experience from the onsite operators and our *in situ* observations including additional noise measurements around the site.

Figure 3 below shows an overview of the site during construction and the main noise sources used in the inverse noise modelling. BH is shadowed in purple, ST in orange, CF in yellow and PB in light red.

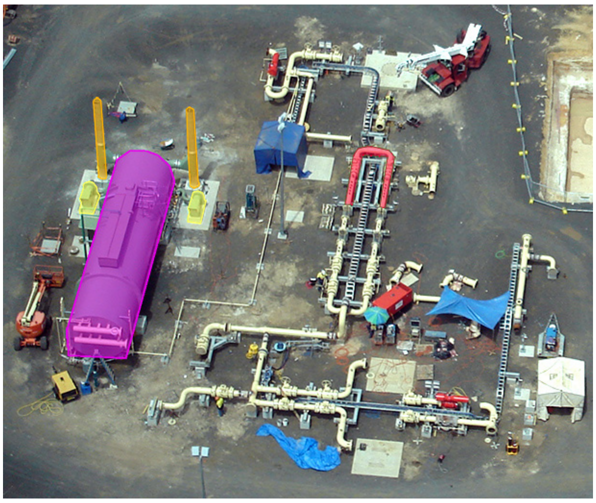

Source: Jemena Asset Management, 2009

Figure 3. Aerial plot of the site during construction

RESULTS

In order to comply with ISO standard 8297 requirements and to facilitate the comparison between the two methods, the results are presented in octave bands. Note that the calculations for both methods can be performed in third octave bands or even narrower filter bands if required.

Two different scenarios were build in CadnaA to accommodate the different input data from the two methods: one scenario with only one noise source power for the ISO standard 8297 and the other one with 10 noise sources for the inverse method. In the later case: point, linear and surface noise sources were used. These models are geo-spatially treated, using the exact same atmospheric conditions and are configured following algorithm procedures contained in [2].

In addition to the real receivers (R1, R2, R3) and for the sake of the explanation, a fictional receiver (see Figure 2, CP) was located closer to plant. The reason being is to illustrate the situation where the noise impact at a potential receiver will have exceeded the recommended criteria.

ISO standard 8297 results

Twenty-nine receiver points along the perimeter of plant area were chosen to carry out the above described methodology for ISO standard 8297. The layout of these receiver points provides the uncertainty inherent in the method, and as per Table 1 in [8], the 95% confidence interval is between +2.0 and -2.5 dB. From these receiver points, the rest of required variables were calculated as follows:

- l = 165 m; perimeter length
- ΔL_f = -1.32 dB; near-field error correction
- S_m = 1575 m^2; measurement area
- S_P = 828 m^2; plant area
- ΔL_S = 33.8 dB; area term

ΔL_α was calculated according to [2] for each octave band and it is almost negligible. Then, the octave band acoustic power values are obtained from following equation

$$L_w = \bar{L}_p + \Delta L_S + \Delta L_f + \Delta L_\alpha \qquad (16)$$

In order to incorporate the acoustic power L_w into CadnaA, the values were introduced to the computer model as a combination of a vertical surface following S_m perimeter with 5 meters height (S_L) plus a plane surface of area S_m, taking into account the areas relation. Table 2 below presents the summary of the resulting surface acoustic power levels in dB (ref. 1 pW); the overall acoustic power level of the whole plant is 105 dBA SWL. Values have been rounded to the nearest integer dB.

Table 2. Acoustic power level of the whole plant divided in two radiating surfaces.

f(Hz)	*32*	*63*	*125*	*250*	*500*	*1k*	*2k*	*4k*	*8k*
$L_w\ S_L$	109	111	107	100	93	92	92	92	88
$L_w\ S_m$	112	114	110	103	96	95	95	95	91

Inverse noise modelling results

Linear operator ***G*(*f*)** was obtained using CadnaA and defining the different noise sources as point (vertical stacks), linear (pipe bendings) and vertical surfaces (centrifugal fans and bath heater). Observation data ***d*** was measured at 64 points in a grid covering the area of S_m using a sound level meter with octave bands filters, following technical advices contained in [9].

Developed scripts under Matlab served to obtain the optimum acoustic power level for each modelled noise source $\boldsymbol{m}_{opt}(\boldsymbol{f})$ This process involved applying Gaussian noise to measured data ***d*** to achieve that 95% of the thousands of new generated values lay in an interval of ±2 dB around the measured values. Table 3 below displays the resulting acoustic power obtained through the inverse modelling.

Table 3. Obtained acoustic power for each noise source, $\boldsymbol{m}_{opt}$

f(Hz)	*32*	*63*	*125*	*250*	*500*	*1k*	*2k*	*4k*	*8k*
PB-1	82	93	94	81	64	84	86	88	75
PB-2	95	96	96	90	83	84	83	89	74
PB-3	95	96	98	83	72	73	94	93	89
PB-4	91	91	76	83	73	76	73	88	79
PB-5	84	99	94	77	83	69	89	88	80
CF-1	92	90	98	90	87	82	80	67	61
CF-2	82	89	96	71	81	81	77	73	66
BH	85	88	92	94	90	93	86	78	72
ST-1	108	108	111	99	97	86	99	97	94
ST-2	106	111	99	104	88	86	89	92	72

Solving the *forward problem* from equation (2) using $\boldsymbol{m}_{opt}(\boldsymbol{f})$ gave us information about the accuracy and the residual errors carried out through the calculations.

Graphical information at each measurement location point is provided using spectrograms for measured and calculated SPL's in following Figure 4. Each measurement location corresponds to each one of the 64 grid points of S_m.

As it can be seen, the main features of the spectra are correctly reconstructed although there is single frequency values were the difference between the measured and the reconstructed differ notably (up to 13dB). The explanation for these differences should be sought in the limitations of the software modelling while building linear operator ***G*(*f*)** in conjunction with the effect of inferences between noise sources and attenuation at high frequencies (2 kHz and 4 kHz).

Until now, we have not been able to find any acoustic procedure in the literature that defines which is the optimum relation between the number of measurements positions and noise sources. This ratio could imply that when the model is unable be accurately reconstructed from measured values, it could be partially attributed to the insufficient spatial information i.e. the model does not have enough measurement location points to capture the correct contribution of each noise source. From this, we could expect to reduce the errors by introducing more measurement locations around the grid taking into account that we should also increase the number of the numerical process iterations to compensate for the *skinniness* of linear operator ***G*(*f*)**.

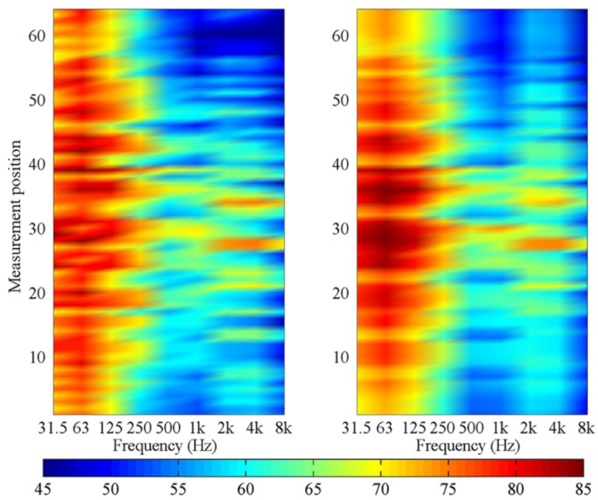

Figure 4. Spectrogram measured dB SPL (left) and calculated dB SPL (right)

However, examination of overall levels reveals that the results are more than acceptable. To ascertain the accuracy of the results additional statistical analysis was carried out. To do so, the errors at each octave band were evaluated. Following Figure 5 displays a summary of the statistical analysis of the error between the measured and calculated data and in form of box-plot.

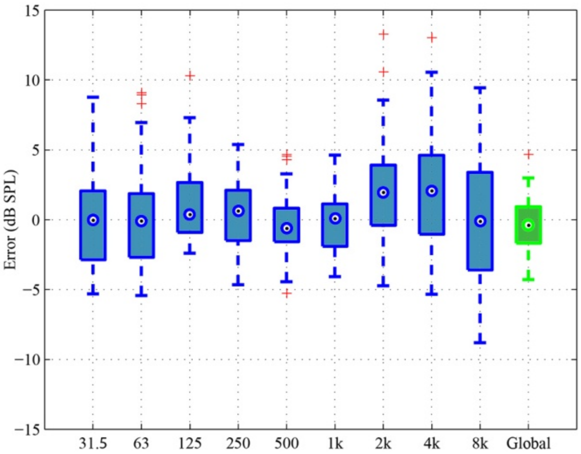

Figure 5. Box-plot error in octave bands (blue) and overall error SPL dBA (green)

According to [17] box-plots are one of the most valuable tool in data analysis. This graph aims to provide the maximum information possible about the errors between the two sets of data (measured and calculated). The data is organised in the following sets: the extremes, the upper and lower hinges (25% and 75% quartiles respectively) and the median. The first incorporates a measure of the group size (max difference between optimum value and the maximum error), the second incorporates an indication of rough significance between medians; the third combines the features of the first two.

In our case it is noticeable that median of the errors at all octave bands is consistently close to zero. At the same time, maximum differences between the extremes are located at either lower or high frequencies. In summary, it seems the mid frequencies are the ones more favourable to be correctly reconstructed. Keep in mind that the A-weighting filter values will smooth the differences particularly at low frequencies. In addition, box-plot graphs could also incorporate outliers (red crosses). According to Moore and McCabe an outlier is an "observation that lies outside the overall pattern of a distribution". In our case we have used a Matlab algorithm to calculate and plot them.

Finally, note that the overall dBA error (see Figure 5, green bar) median is 0 with 25% quartile at -1.6 dBA and 75% quartile at 0.9 dBA, thus giving 2.6 dBA with a 50% confidence interval. Moreover, we can see a maximum of 3 dBA, a minimum of -4 dBA and only one single outlier has been detected, i.e. the overall calculated dBA value differs only one of the 64 points from the measured more than 3 dBA.

Comparison

Table 4 displays a summary SPL values that have been obtained using the two different CadnaA scenarios:

Table 4. SPL $L_{Aeq(15min)}$ dBA results comparison.

	R1	*R2*	*R3*	*CP*
ISO 8297	23	21	28	44
Inv. Model	24	20	26	42

As it can be seen in Table 4, there are small differences between the two methods. These differences are attributed to the way the acoustic power levels are incorporated into the model and to the directivity pattern from the different noise sources. For ISO standard 8297 scenario, one single value is divided into two different radiating surfaces (see Table 2) while in the inverse model scenario, we have 10 different noise sources with their specific directivity pattern and their real location (see Table 3). Because of these differences, it is understandable that the results at a far field have differences up to 2 dBA SPL. It is also visible that the results from both methods will comply with the applicable criteria at the residential receivers R1, R2 and R3. Notwithstanding that, we have deliberately selected a control point CP to illustrate what could have happened in another scenario if the residential receivers would have been located closer to the industrial plant. At the control point CP, predictions from both methods exceed the criteria values at R2 and R3; it is precisely in this situation where the inverse noise model provides a clear advantage in front of the ISO standard 8297. Actually, at any given point of our inverse model we will be able to list, rank and quantify the contributions in noise levels of each single noise source. This is clearly useful when trying to define solutions.

Figure 6 below shows a summary of the noise sources contributions at control point CP. In this particular location, the pair of stack exhaust is the main contributor to the overall noise. Thus, in the event that CP would have been a real receiver the engineering efforts should have been directed in designing a silencer system that reduced by 5 dB the contribution of each stack achieving then the required 40 dBA SPL at any receiver location. Meanwhile, CF-2 is the smallest noise contributor at this receiver point due to the water bath heater (BH) acting as a barrier.

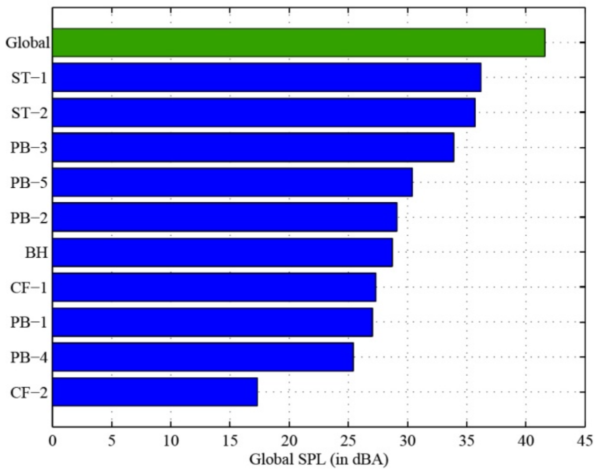

Figure 6. Individual noise source contributions in SPL dBA at control point receiver (blue), and overall SPL dBA (green)

CONCLUSIONS

A noise propagation inverse theory model has been developed as an alternative method to improve ISO standard 8297. A noise survey in an industrial plant was conducted following the two methods and the data was later retrieved and used in two different noise propagation software models according to the two described methodologies. Similar results were obtained using both methods although inverse noise modelling was proved more valuable when solutions were required.

ISO standard 8297 converts all noise sources to a single acoustic power, assumes a noise pattern directivity related with the shape of S_m and the dimensions of industrial plant are constrained by the standard definitions. Therefore, the procedure inabilities the possibility of identifying any individual noise sources if further measured are required. On the contrary, inverse theory modelling solves these restrictions and it can not only define the noise sources but also rank them and quantify them providing with a much valuable information.

Because of the way that ISO standard 8297 is defined, *the radiating box* radiates noise towards the exterior of the plant, there is no mention to the interior of the facility in the standard, thus, it is not valid to perform any Occupational, Health and Safety (OH&S) measurement. Inverse noise model is suitable for performing OH&S measurements because it achieves the reconstruction of the near field of all noise sources allowing noise hazardous zoning definition by means of ranking the influence area of each noise source.

In terms of time consumption while performing the measurements, we believe both methods are similar although the dimensions of the site plus the number of sources will determine which method is faster. Note that ISO standard 8297 will require previous work on defining the measurement points beforehand while the inverse model will rely on the *in situ* observations and the physical configuration of the plant. The post processing of the data (obtaining ***G***) is clearly more time demanding in the inverse modelling because it requires individual noise source modelling while the ISO standard 8297 could be performed by hand or using a simple spreadsheet. However, we are the opinion that the benefits of the inverse model justify the handicaps of the method and clearly surpasses the ISO standard 8297 results.

No mention has been done to the limitations of the computer software modelling because, in that instance, both methods are equally affected (both of them use CadnaA). Information about this matter can be found in [18].

Finally, the main drawback of using the inverse noise modelling is that it is not an officially recognized standard and therefore it will be only applicable under explicit customer's endorsement.

Future work

We believe inverse noise modelling has great potential in solving many of the problems in the industrial noise environments. At the same time, we are aware that there are several issues that could be improved such as:

- Including far field measurements for building ***G***.
- Changing the strategies to minimize the outliers, i.e. improving the probabilistic approach to ease the way the errors are evaluated.
- Investigate the adequacy of the method when using large numbers of noise sources; will it be feasible with five hundred noise sources?
- Refining computational time by means of iterations needed to achieve a stable solution.

Finally, although the theory is in our favour we would like to evaluate the inverse noise modelling method in an indoor scenario where the room characteristics such as absorption coefficients and reverberation time will play an important role in defining the linear operator ***G***.

Another interesting application of inverse noise modelling could be the automated dynamic noise mapping. i.e. a noise map that can be updated in predefined time intervals using measured data. The most important application of this system could be the direct coupling of the model to an automatic monitoring system installed along main roads or near industrial plants. Once the inversion noise modelling is complete, remote data is send from the monitors to the main computer allowing an almost real time contributions list of all the noise sources involved in our model.

Acknowledgements

The authors wish to thank *Jemena Asset Management Pty Ltd.* for their support and grant permission to publish measurement data and to Dr. Guasch and our colleagues at *Ingeniería para el Control del Ruido* (ICR) for their introduction to the world of inverse theory.

REFERENCES

1 Cuevas-Cubria C, Penney K, Schiltz A, "Energy in Australia 2009". *Department of Resources Energy and Tourism, Australian Government* (2009).

2 ISO 9613, "Attenuation of sound during propagation outdoors -- Part 1: Calculation of the absorption of sound by the atmosphere; Part 2: General method of calculation", *International Standards Organization, Genève, Switzerland* (1996).

3 DIN 45635, Part 47, "Measurement of noise emitted by machines; airborne noise emission; enveloping surface method; chimneys" *Deutsches Institut für Normung,* Berlin, Germany, (1985).

4 VDI 2714, "Outdor sound propagation", *Verein Deutscher Ingenieure,* (1988-1).

5 Luzzato E. Application of the ray tracing technique to sound source identification. In: *Proceedings of internoise*, Munich, Germany, September 1985. p. 1235–8.

6 Luzzato E, Lecointre C. Some simple and effective methods for sound source identification with geometrical acoustic models. *J Sound Vib* 1986;105(3):473–90.

7 Guasch O., Magrans F.X., Rodriguez P.V., "An inversion modelling method to obtain the acoustic power of the noise sources in a large factory", *Applied Acoustics 63 (Elsevier Science Ltd., 2002)* pp. 401-417.

8 ISO 8297, "Determination of acoustic power levels of multisource industrial plants for evaluation of sound pressure levels in the environment – Engineering method", *International Standards Organization, Genève, Switzerland,* (1994).

9 ISO 1996, "Description, measurement and assessment of environmental noise. Part 1: Basic quantities and assessment procedures; Part 2: Determination of environmental noise levels", *International Standards Organization, Genève, Switzerland,* (2003, 2007).

10 Blake S., Teague P., "Prediction of long range propagation of peak overpressure from blast events". Annual Conference of the Australian Acoustical Society, Adelaide, Australia, (November 2002).

11 Brittain F.H., "Using ISO 8297 to verify community noise requirements given as limits on acoustic power levels". *Institute of Noise Control Engineering*, Noise-Con (2007).

12 Tapan K. Sarkar, et al, "Some mathematical considerations in dealing with inverse problems". *IEEE Transactions on Antennas and propagation*, Vol AP-29, NO. 2. March 1981.

13 Hansen. C., "Regularization tools, A Matlab package for analysis and solution of discrete ill-posed problems, v4.1". *Numerical algorithms 46*. pp 189-194 (2007).

14 Tarantola, A. "Inverse Problem Theory and Methods for Model Parameter Estimation", *Society for Industrial and Applied Mathematics*, (2005).

15 Klaus Mosegaard and Albert Tarantola. "International Handbook of Earthquake and Engineering seismology (Part A)" in "*Probabilistic approach to inverse problems*", ed. Academic Press, pp 237-265, (2002).

16 H. Läuter and H. Liero "Ill-posed inverse problems and their optimal regularization" *Deutsche Forschungsgemeinschaft* (July 1997).

17 McGuill, R., J.W.Tukey and W.A.Larsen. "Variations of Boxplots". *The American Statistician*. Vol. 32, No. 1, pp 12-16 (1978).

18 Brittain F.H., Marlund E.H., "Some Limitations of Ray-Tracing Software for Predicting Community Noise from Industrial Facilities". *Institute of Noise Control Engineering*, Noise-Con (2008).